3D printing of topological composites by photopolymerization from submicron piezoceramics

© T. Arshad[1], O.N. Dubinin[1], I.V. Shishkovsky[1,2]

[1] Skolkovo Institute of Science and Technology, Moscow, Russia
[2] Lebedev Physical Institute, Samara Branch, Russian Academy of Sciences, Samara, Russia
E-mail: shiv@fian.smr.ru

A new scalable approach to the design and 3D printing of green part topological composites from lead titanate zirconate powder (PZT) or barium titanate (BaTiO3) for the manufacture of low-density piezoelectric products for medical or hydrological applications has been implemented. Ceramic polymer suspensions with a content from 13% to 50% vol of piezoceramics of submicron sizes were prepared and their printing regimes were optimized. The densities of 3D green parts solid sound $(0-3)$ and lattice $(1-3)$, $(3-3)$ 3D samples were determined by the Archimedes method.

Keywords: hierarchical lattice structures, lead titanate zirconate, barium titanate, UV vat polymerization, digital light processing (DLP)

Piezoceramic materials have a wide range of applications as sensors or actuators [1]. Traditional piezoceramics processing techniques include dry pressing, belt casting, and roll forming. However, traditional methods are ill-suited for production of electronic devices with a complex geometry from ceramic materials [2]. At the same time, the shape of parts and the density of piezoceramics may affect their functional properties, such as the coefficient of matching with the studied medium, directly. Additive manufacturing (AM) provides flexibility and control over the geometry, shape, size, density, and piezoelectric and mechanical properties of 3D-printed parts. The use of AM opens up broad prospects for fabrication of piezoelectric materials with a complex geometry and a new set of piezo- and dielectric properties [1] and also allows one to adjust the necessary characteristics of materials in accordance with their functional purpose.

UV polymerization (UVP), which provides an opportunity to produce ceramic structures and devices of a complex shape with a high resolution from a digital model, is one of the key AM approaches [1]. The viscosity of suspensions used for UVP depends on the volume and composition of the filler and exerts a direct influence on the quality of 3D printing and the resulting characteristics of manufactured parts. Such products are in demand in the production of specialized sensors used in marine acoustics, seismology, medical ultrasound diagnostics [2–5], etc. Polymer ceramic composites (PCCs) have an additional advantage in providing an opportunity to raise the mechanical strength of the material while simultaneously reducing its density [4]. The discussed engineering solutions for 3D printing of piezoceramics are relevant to the production of hierarchical lattice structures (HLSs) with topological connectivity [1,4].

An original and scalable approach to fabrication of lattice topological structures from PCCs based on lead zirconate titanate (PZT) or barium titanate (BT) is presented below. The lack of lead in BT would undoubtedly be an advantage in medical applications.

PZT-5H and $BaTiO_3$ piezoceramic powders and UV resin (Harz Labs) were produced in Russia. PZT and BT were synthesized using the traditional solid-phase synthesis method at the Moscow Polytechnic University [1,6]. The mean particle size of PZT powders was in the submicrometer range: 10, 5, 3.5, and $1-2\,\mu m$ with a considerable amount of satellite nanoparticles with a diameter of $\sim 0.5\,\mu m$ (or smaller). According to scanning electron microscopy (SEM) data, the BT powder had a mean particle size (D_{50}) of $\sim 0.25\,\mu m$ (Fig. 1). It can be seen that the shape of PZT particles was highly irregular. Nanosized BT particles had a high degree of sphericity, and their packing after sintering could be quite dense. Various compositions of PCCs (pastes) were prepared to study their rheological properties and determine the UVP depth and the times of their degradation in the course of storage. No additional inhibitors, plasticizers, or dispersants were introduced into the suspensions. A total of 28 pastes with PZT concentration $\varphi = 13, 18, 26, 30, 37, 45,$ and $50\,\text{vol.\%}$ were prepared with the use of PZT particles of four different sizes indicated above. As for the BT powder, pastes with a BT concentration of $13-37\,\text{vol.\%}$ were prepared. The density of the initial PZT and BT ceramics was $7.5\,\text{g/cm}^3$ and $6.03\,\text{g/cm}^3$, respectively, and the resin density specified by the supplier was $1.1\,\text{g/cm}^3$. The weight of PCCs was monitored thoroughly and measured with a Galaxy HR-250AZ analytical balance. Following mixing, the PCCs were introduced into a vacuum chamber (Struers Citovac)
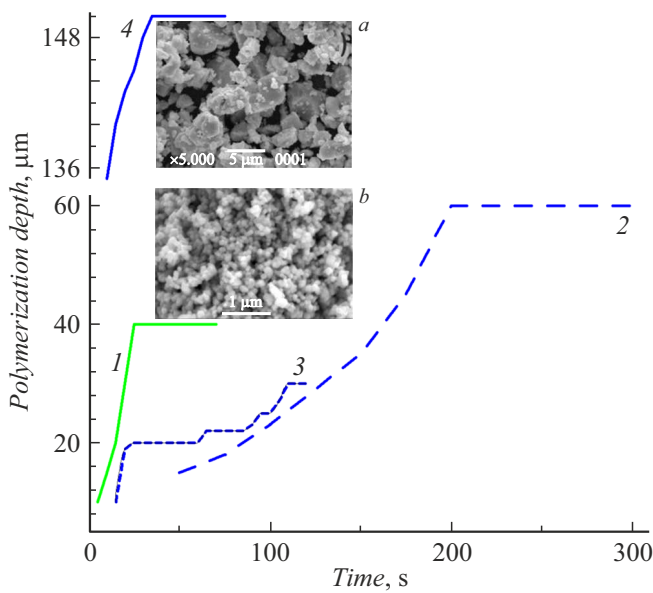
Figure 1. Photopolymerization depth of 3D samples of pastes with BT and PZT as a function of exposure time. *1* — 37 vol.% BT, the mean ceramic particle size is $0.25\,\mu$m; *2* — 50 vol.% PZT, $2\,\mu$m; *3* — 37 vol.% PZT, $3.5\,\mu$m; *4* — 37 vol.% PZT, $5\,\mu$m. SEM images of the initial piezoceramic powders are shown in the insets: PZT (*a*) and BT (*b*).

to remove any air that had become entrapped in the paste in the process of mixing. A Phrozen Sonic 8k Mini (China) projection 3D printer with an open source *G*-code, which performs layer-by-layer 2D-masked UV illumination of the paste (digital light processing (DLP) method implemented with an LED module operating at wavelength $\lambda = 405$ nm), was used for printing. After curing, the parts were dried in an oven at a temperature of $60°$C for 3 h to remove residual moisture. The dimensions were determined with a caliper (the measurement error was 0.5 mm), and the weight and density of samples were calculated by the Archimedes method using an OHAUS Pioneer™ density analyzer (OHAUS Instruments Co., Shanghai) with an error level of ±0.06.

Polymerization depth C_d was recorded at different exposure times to determine the maximum curing range of suspensions for all filler compositions by volume. C_d depends on the conditions of absorption and scattering of UV radiation by the ceramic powder in the resin and is characterized by the modified Bouguer−Beer equation:

$$C_d = \frac{2\lambda D_{50}}{3\varphi h \Delta n^2} \ln \frac{E}{E_c}, \qquad (1)$$

where E and E_c are the applied and critical irradiation doses, h is the distance between powder particles, and Δn is the difference between the refraction indices of the ceramic powder and the UV resin. The absorbance of commercial PZT and BT powders is 0.37 and ~ 0.25, while the absorbance of pastes is ~ 0.22 in UV radiation with a wavelength of 405 nm [1,7].

Figure 1 presents the results for compositions with the maximum PZT or BT concentration from the studied range. All plots (*1–4*) reach a saturation level where a further increase in exposure time becomes inexpedient. Overexposure may extend the printing process and cause more light scatter, resulting in the production of parts with dimensions greater than those specified in the CAD (computer-aided design) model. Underexposure may result in incomplete polymerization of layers or detachment of the initial layer from the mold plate or the preceding layer (in multilayer printing). The optimum layer thicknesses for each type of paste with the highest concentration of ceramic filler were determined. Experiments revealed that only one half of the total layer height is utilized in the PCC printing process. Therefore, it was recommended for multilayer 3D printing with overlap to assume that the second half of the total curing depth ensures a sufficient margin of adhesion strength in the optimum range of curing depths of each preceding layer.

The mean particle sizes of ceramics are indicated in the caption of Fig. 1. A comparison of the presented plots reveals that a smaller particle size and a higher filler (PZT or BT) concentration in the suspension reduce the curing depth significantly and require longer exposure times, but increase the resolution of 3D-printed parts. It is possible to achieve stable UVP for 50 vol.% BT [7], but inhibitors need to be added to the paste, and laser radiation is better suited for illumination in this case. Both the shape of the piezoceramic powder (see Eq. (1) and Fig. 1) and the degree of packing of ceramic particles in the suspension affect the UVP depth [7,8]. Submicrometer and nanosized particles (inset *b* in Fig. 1) make the paste more stable in printing and eliminate the problem of suspension sedimentation over time. Pastes containing PZT particles $5-10\,\mu$m in size (inset *a* in Fig. 1) allow for polymerization depths up to $150-200\,\mu$m or more, but this has a negative effect on the resolution of 3D printing.

Submicrometer pastes had fine rheological parameters (i.e., filled each subsequent layer within the interval of platform motion in the process of printing and remained suitable for use for several weeks without any signs of separation of the ceramics from the resin). Our earlier measurements [7] of the dependence of viscosity on shear rate revealed pseudoplastic behavior of pastes. The reduction of their viscosity with an increase in shear rate may be attributed to disruption of the tangled structure of polymerized resin. Suspensions with particles larger than $5-10\,\mu$m settled faster, and the ceramic powder got deposited on the bottom of the bath, blocking UV radiation, restricting the motion of the molding plate, and eventually causing failure of the 3D printing process. One needs to choose proper dispersants to eliminate this problem (see [2,3,7,8]).

Different types of HLSs were prepared using the Materialize Magic software (version 25.0.2.435). Figures 2, *a−c* present the HLSs fabricated from PCCs based on 50 vol.% PZT with particles $2\,\mu$m in size, and the sample based on 37 vol.% BT with particles $0.25\,\mu$m in size is

Geometric parameters of HLSs with topological connectivity

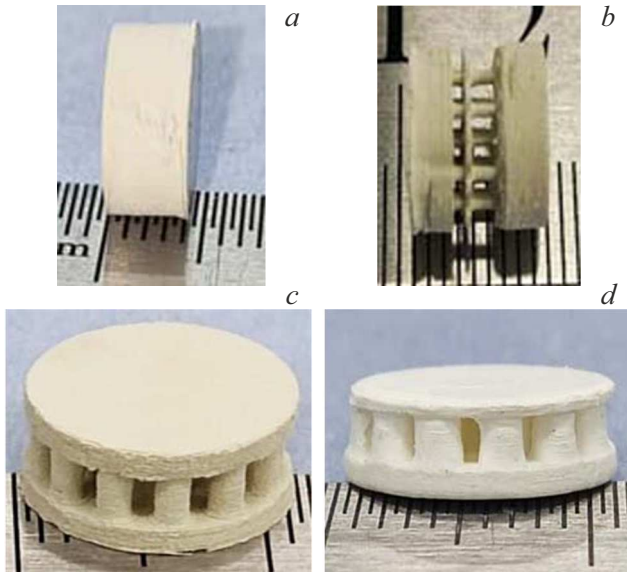| Material and connectivity type	Overall time, min	Layer height, μm	Density, g/cm^3	ε_H, %	ε_D, %
50 vol.% PZT, solid sample $(0-3)$	88.7	15	2.81	0.08	-0.02
PZT, ladder structure $(3-3)$	133.3	40	4.56	0.09	-0.02
PZT, rod structure $(1-3)$	35.7	25	4.41	0.1	0.06
37 vol.% BT, solid sample $(0-3)$	8.8	15	5.2*	0.13	-0.02
BT, rod structure $(1-3)$	7.5	20	5.0*	0.18	0.09

* Subject to additional verification.

Figure 2. External view of 3D-printed HLSs with different types of topological connectivity. *a* — Solid PZT $(0-3)$, *b* — PZT $(3-3)$, *c* — PZT $(1-3)$, and *d* — BT $(1-3)$. The ruler scale interval is 1 mm.

shown in Fig. 2, *d*. The diameter of samples was set to 11 mm. Cylindrical HLSs with topological connectivity types $(1-3)$ and $(3-3)$ featured top and bottom solid sections, each with a thickness of $\sim 1-1.5$ mm, and a middle section with a vertical HLS (Figs. 2, *b*–*d*). The HLS $(3-3)$ sample has a clearly visible detachment defect. In addition to lattice structures, solid cylindrical samples (Fig. 2, *a*) in the form of a pellet with its height and diameter similar to those of the HLSs were fabricated for comparison. Admittedly, according to the generally accepted Newnham classification [1,4], they may also be regarded as a topological structure $(0-3)$.

The overall time of 3D printing and the optimized height of each layer are listed in the table. The density of PZT was determined after fabrication and drying in a UV box. The values averaged over five samples are presented in the table. It can be seen that this density for the solid pellet (Fig. 2, *a*) and HLSs (Figs. 2, *b, c*) is just ~ 0.4 and ~ 0.6 of the reference PZT density, respectively. The counterintuitively lower (relative to the HLS samples) density of the solid pellet may be attributed to the effects of light scattering off PZT particles, which is more intense in the $(0-3)$ structure than in the $(1-3)$ or $(3-3)$ structures. It is evident that the dimensions of 3D-printed samples are greater than those specified in the CAD model. The table presents estimates of the relative experimental change in height (ε_H) and diameter (ε_D). While the average height enhancement is uniform ($\varepsilon_H \sim 0.1\%$), the diameter could both increase and decrease after printing. Compression was observed mostly in solid $(0-3)$ samples.

The following conclusions were made based on the obtained data. Submicrometer and nanosized ceramic powders are recommended for 3D printing and allow one to achieve high concentrations of PZT and BT in PCCs with the use of low-cost DLP technology and without any additives. The particle size of piezoceramics is of paramount importance for the stability of rheological properties of pastes without plasticizers. The optimum particle size ($1-2\,\mu m$ or smaller) ensures high concentrations of ceramic powders in a suspension: up to 50 vol.% for PZT and 37 vol.% for BT. Suspensions with higher concentrations of piezoceramics had smaller UVP depths ($\sim 40-50\,\mu m$) and required longer exposure times. 3D-printed HLS parts with topological connectivity types $(0-3)$, $(1-3)$, and $(3-3)$ have been obtained for the first time, which should provide an opportunity to increase the output power of devices based on them.

Acknowledgments

Conflict of interest

The authors declare that they have no conflict of interest.

References

[1] A. Smirnov, S. Chugunov, A. Kholodkova, M. Isachenkov, A. Vasin, I. Shishkovsky, Ceram. Int., **47** (8), 10478 (2021). DOI: 10.1016/j.ceramint.2020.12.243

[2] J. Ye, H. Gong, Y. Zhang, Q. Xu, X. Zhou, M. Yan, D. Zhai, K. Zhou, D. Zhang, C. Bowen, Addit. Manuf., **79**, 103915 (2024). DOI: 10.1016/j.addma.2023.103915

[3] S. Chang, S. Hur, J. Park, D. Lee, J. Shin, H.S. Kim, S.E. Song, J.M. Baik, M. Kim, H.C. Song, C.Y. Kang, Addit. Manuf., **67**, 103470 (2023). DOI: 10.1016/j.addma.2023.103470

[4] E. Tarasova, I. Juravleva, I. Shishkovsky, R. Ruzhechko, Phase Trans., **86** (11), 1121 (2013).
DOI: 10.1080/01411594. 2013.803105

[5] Z. Jiang, L. Cheng, Y. Zeng, Z. Zhang, Y. Zhao, P. Dong, J. Chen, Ceram. Int., **48** (5), 6477 (2022).
DOI: 10.1016/j.ceramint.2020.12.243

[6] A.V. Smirnov, A.A. Kholodkova, M.V. Isachenkov, M.V. Kornyushin, I.V. Shishkovskii, Glass Ceram., **79** (7–8), 312 (2022). DOI: 10.14489/glc.2022.08.pp.028-042

[7] A. Tikhonov, S. Chugunov, I. Shishkovsky, Opt. Spectrosc., **130** (10), 1555 (2022).
DOI: 10.21883/OS.2022.10.53625.3825-22 [A. Tikhonov, S. Chugunov, I.V. Shishkovsky, Opt. Spectrosc., **130** (10), 1297 (2022). DOI: 10.21883/EOS.2022.10.54866.3825-22].

[8] K. Liu, C. Zhou, J. Hu, S. Zhang, Q. Zhang, C. Sun, Y. Shi, H. Sun, C. Yin, Y. Zhang, Y. Fu, J. Eur. Ceram. Soc., **41** (12), 5909 (2021). DOI: 10.1016/j.jeurceramsoc.2021.04.044

Translated by D.Safin